Protein structure change studied by hydrogen-deuterium exchange, functional labeling, and mass spectrometry

Joan J. Englander*†, Charyl Del Mar*, Will Li*, S. Walter Englander*‡, Jack S. Kim§, David D. Stranz¶, Yoshitomo Hamuro‖, and Virgil L. Woods, Jr.‡§

*Department of Biochemistry and Biophysics, University of Pennsylvania, Philadelphia, PA 19104; §Department of Medicine, University of California at San Diego, La Jolla, CA 92093; ¶Sierra Analytics, LLC, 2105 Lancey Drive, Suite 1A, Modesto, CA 95355; and ‖ExSAR Corporation, Monmouth Junction, NJ 08852

Contributed by S. Walter Englander, April 17, 2003

An automated high-throughput, high-resolution deuterium exchange HPLC-MS method (DXMS) was used to extend previous hydrogen exchange studies on the position and energetic role of regulatory structure changes in hemoglobin. The results match earlier highly accurate but much more limited tritium exchange results, extend the analysis to the entire sequence of both hemoglobin subunits, and identify some energetically important changes. Allosterically sensitive amide hydrogens located at near amino acid resolution help to confirm the reality of local unfolding reactions and their use to evaluate resolved structure changes in terms of allosteric free energy.

Hydrogen exchange (HX) measurements can, in principle, locate protein-binding sites and structure changes and can quantify otherwise unavailable dynamic and energetic parameters (1–4). For relatively small proteins, HX can be measured at an amino acid resolved level by NMR methods. For larger, functionally more interesting proteins, other strategies are required. Earlier work (5, 6) developed a "functional-labeling" approach that can selectively label, by hydrogen-tritium (H-T) or hydrogen-deuterium (H-D) exchange, just those sites that change in any functional process. In favorable cases, the label can then be located at medium resolution by a proteolytic fragmentation method in which the fragments are quickly produced and then separated by HPLC under conditions where the loss of isotopic label is slow (6–9).

To move toward higher resolution and more comprehensive coverage of target proteins, recent work in many laboratories has coupled the HPLC separation to a second dimension of fragment resolution by online MS (10, 11). These methods tend to be labor intensive and time consuming, with limitations in throughput and comprehensiveness and in the structural resolution of functionally important changes. This article merges previous HX functional labeling and fragment separation methods with an automated MS approach termed deuterium exchange MS (DXMS) (12–18).

We are using Hb as a model system to study how protein molecules manage intramolecular signal transduction processes. Hb functions by transducing a part of the binding energy of its initially bound O_2 ligands into structure-change energy. The energy is carried through the protein to distant heme sites in the form of energetic structure changes, and there transduced back into binding energy. The initial reduced binding energy and the later enhanced binding produces the physiologically important sigmoid binding curve. In short, the currency of allosteric interactions is free energy. Trying to understand allostery without measuring free energy is like trying to understand an economic system without measuring money. A great deal of information on regulatory structure change in many proteins is now available, but mainly in a qualitative pictorial sense from "before and after" crystallographic or NMR views. How these changes participate in energy transduction and translocation has been little explored (19–22).

The HX work described here is directed toward the goal of specifying the individual allosterically important structure changes, the energetic contribution of each, and how they interact to produce the allosteric function. The methods used here provide complete protein coverage, nearly site resolution, and high-throughput efficiency. The results obtained compare well with previous highly accurate but more limited H-T exchange results and specify the position and energetic contribution of several allosterically important changes through the Hb molecule. We also consider the issue of concerted unfolding vs. local fluctuational HX processes and their significance for measuring the free energy of structure changes.

BIOPHYSICS

Methods

Hb. Human Hb was prepared from fresh red cells by standard methods and was stored frozen at −80°C. Deoxygenation used argon bubbling, dithionite, a glucose oxidase-catalase mixture, and ferrous pyrophosphate (23, 24), which also acts as a T state-selective bisphosphoglycerate analog.

Functional Labeling and Analysis. Initial isotopic labeling of Hb with tritium or deuterium was done by limited exchange-in under the conditions specified. To initiate exchange-out, Hb samples were transferred into H_2O buffer by gel filtration (Sephadex G-25 fine/0.1 M phosphate, pH 7.4/0°C/0.1 M NaCl) by using low-pressure-driven columns or centrifugal spin tubes (25).

For the fragment separation analysis, timed exchange-out samples were quenched into slow HX conditions [gel filtration, 1% trifluoroacetic acid (TFA) adjusted to pH 2.3 with NH_4OH, 0°C/50 mM GdmCl/10% glycerol to promote later sample thawing at 0°C], then were deep-frozen (−80°C) in autosampler vials pending analysis at the DXMS Proteomics Resource (Department of Medicine, University of California at San Diego). Samples were automatically thawed and analyzed by using online proteolysis with immobilized enzymes, followed by reverse phase HPLC/MS under slow HX conditions (pH 2.3, 0°C).

Loss of D-label by individual fragments during the DXMS analysis was calibrated by using Hb samples that were initially fully labeled by incubation under unfolding conditions (pD 2.3), and then moved into H_2O solution before proteolysis as was done for experimental samples. Loss corrections were made as described (Table 1).

Results shown here were obtained over a period of time by using several different MS systems. Agreement was generally excellent. The most current methodology is described.

Fragment Identification. For each digestion condition used, data were acquired by parallel MS1 acquisition and data-dependent

Abbreviations: HX, hydrogen exchange; DXMS, high-throughput, high-resolution deuterium exchange HPLC-MS; TFA, trifluoroacetic acid.

†Deceased June 17, 2000.

‡To whom correspondence may be addressed at: Department of Biochemistry and Biophysics, University of Pennsylvania School of Medicine, Philadelphia, PA 19104-6059. E-mail: walter@hx2.med.upenn.edu; or Department of Medicine, University of California at San Diego, 9500 Gilman Drive, BSB 5078, La Jolla, CA 92093. E-mail: vwoods@ucsd.edu.

MS2 acquisition with dynamic exclusion. The SEQUEST software program (Thermo Finnigan, San Jose, CA) identified the likely sequence of the parent peptide ions. Tentative identifications were tested with specialized DXMS data-reduction software developed in collaboration with Sierra Analytics. This software searches MS1 data for scans containing each of the peptides, selects scans with optimal signal/noise, averages the selected scans, calculates centroids, screens for peptide misidentification by comparing calculated and known centroids, then facilitates visual review of each averaged isotopic envelope, allowing an assessment of "quality" (yield, signal/noise, and resolution) and confirmation or correction (16–18).

Equipment Configuration. The equipment configuration consisted of electrically actuated high-pressure switching valves (Rheodyne, Cotati, CA) connected to two position actuators (Tar Designs, Pittsburgh), except for a six-position valve-actuator multicolumn selection assembly (Valco Instruments, Houston; ref. 16). A highly modified AS3000 autosampler (Spectra-Physics), partially under external PC control, lifts the desired frozen sample from the sample well, then automatically melts and injects it under precise temperature control (13, 17, 18). The autosampler basin was further thermally insulated, and all but 20 vial positions were filled with powdered dry ice, which was sufficient to keep samples colder than −45°C for 18 h.

Four Shimadzu LC-10AD HPLC pumps were operated by a Shimadzu SCL-10A pump controller. One drives the protease columns, another backflushes after sample digestion (0.05% aqueous TFA), and two deliver solvents to a downstream HPLC column for gradient elution [Solvent A: 0.05% aqueous TFA; Solvent B: 80% acetonitrile, 20% water, 0.01% TFA, pH 2.3; 1 × 50 mm C18 Vydac (Hesperia, CA)]. The valves, tubing, columns, and autosampler were contained within a refrigerator at 2.8°C, with HPLC columns immersed in melting ice.

The timing and sequence of operation of the DXMS fluidics were PC controlled, running an inhouse-written LABVIEW-based program, interfaced to solid-state relays [digital input/output boards, National Instruments (Austin, TX)], controlling pumps, valve actuators, and MS data acquisition. The integrated automation of fluidics allows continuous data acquisition at 30 min per sample.

DXMS Analysis. For analysis, samples were placed in the dry ice-containing sample basin of the autosampler, individually melted, then injected (45 μl) and pumped through the protease columns (0.05% TFA, 250 μl/min, 16-sec protease exposure). Proteolysis used immobilized pepsin alone or pepsin followed by *Aspergillus saitoi* fungal protease type XIII [EC 3.4.23.6, Sigma; 66-μl column bed volume, coupled to 20AL support from PerSeptive Biosystems (Framingham, MA) at 30 mg/ml]. The samples were collected onto the C18 HPLC column, eluted by a linear acetonitrile gradient (5–45% B in 10 min or 30 min; 50 μl/min), and injected directly into the mass spectrometer run in either MS1 profile mode or data-dependent MS2 mode. MS analysis used Thermo Finnigan LCQ electrospray ion trap type mass spectrometer operated with capillary temperature at 200°C or an electrospray Micromass (Manchester, U.K.) Q-TOF mass spectrometer (16–18).

Stabilization-Free Energy. Amide hydrogens protected by protein molecular structure exchange slowly with solvent, at rates that are determined by the small fraction of time that the structural protection (H-bonding) is lost in some transient dynamic "opening" reaction (26, 27), as in Eq. **1**. The complex steady-state expression for HX rate usually simplifies to Eq. **2** (hydroxide-catalyzed above pH ≈4). The so-called EX2 region (bimolecular exchange; Eq. **2**), where HX rate (k_{ex}) depends on the structural opening equilibrium constant, K_{op}, and pH, generally holds below pH ≈10. The term k_{int}, the intrinsic second-order HX rate constant calibrated for unprotected amides (28, 29), is applicable when amide hydrogens are freely exposed to solvent, e.g., in a concerted unfolding reaction, but perhaps not when exchange occurs by way of more constricted local fluctuations (30). When Eq. **2** is valid, the free energy of unfolding reactions that determine exchange rates, dependent on local structural stability, can be expressed in terms of measured HX rate (k_{ex}) as in Eq. **3**. When some change produces a change in structural stabilization free energy, and therefore in HX rate, these relationships translate into Eq. **4** (assuming that the open state is at the same free energy in both forms).

$$\text{closed} \underset{k_{cl}}{\overset{k_{op}}{\rightleftharpoons}} \text{open} \xrightarrow{k_{ch}} \text{exchange:} \qquad K_{op} = k_{op}/k_{cl}, \qquad [1]$$

$$k_{ex} = K_{op}\, k_{int}[OH^-] = K_{op}\, k_{ch}, \qquad [2]$$

$$\Delta G_{op} = -RT \ln K_{op} = -RT \ln(k_{ex}/k_{ch}), \qquad [3]$$

$$\Delta\Delta G_{op} = -RT\, \Delta \ln K_{op} = -RT \ln(k_{ex,1}/k_{ex,2}). \qquad [4]$$

Results

HX Progression. Fig. 1 recapitulates the increasing resolution of HX studies by using the Hb example. Fig. 1*A* shows H-T exchange results for Hb at an unresolved whole-molecule level. Hb labeled to exchange equilibrium in tritiated water was exchanged out in the oxy (R state) and deoxy (T state) forms. Some allosterically sensitive hydrogens exchange faster in oxy Hb than in deoxy Hb. In this mode, the number of sensitive hydrogens and their HX rates in either protein form cannot be determined because of the large background of unresolved sensitive and insensitive hydrogens that exchange over a wide range of time scales.

A functional labeling method illustrated in Fig. 1*B* focuses HX labeling on only the sites that change. The fast-exchanging oxy Hb form was partially labeled by exchange-in in tritiated water for a limited period (1 min in this case). Allosterically sensitive and insensitive sites that exchange in this time period become labeled. The Hb sample was then switched to the slow-exchanging deoxy form and moved into untritiated solvent (gel filtration, <1 min). The bound label begins to exchange-out. After some exchange-out (chase) time, label on allosterically insensitive sites (same HX rate in both forms) is largely lost, but it is retained on allosterically sensitive sites, which are slowed in deoxy Hb. Thus, the exchange-in/exchange-out sequence produces a sample with label selectively placed on functionally sensitive sites (6, 31). HX measurement then reveals the number of sensitive residues and their HX rates in both forms.

A correction for the residual background due to allosterically insensitive sites that still contribute to the HX curve (especially at early exchange-out time) can be made by doing the selective labeling in the reverse direction (exchange-in deoxy, exchange-out oxy) to obtain a curve that largely shows the residual background-insensitive hydrogens. Subtraction of the background curve yields an HX curve essentially for the sensitive sites alone (Fig. 1*B Inset*). Two sets of allosterically sensitive hydrogens exchange more slowly in deoxy Hb by almost 1,000-fold and 10,000-fold. Selectivity and accuracy increase with the rate difference, i.e., with the importance of the structure change, and decrease to zero as the rate difference disappears.

A fragment separation method can then identify the positions of the selectively labeled allosterically sensitive sites at medium resolution (6–9). Samples taken after different exchange-out times are plunged into slow HX conditions (pH ≈2.5, 0°C) and quickly fragmented with acid protease. The fragments are separated under slow HX conditions and then analyzed for carried label. Fig. 1*C* shows results obtained by tritium exchange (circles) for a set of amides located on an N-terminal fragment of the α-chain (α1–29). Fig. 1*D* shows another set near the β-chain C terminus (on β130–146), which appears to account for

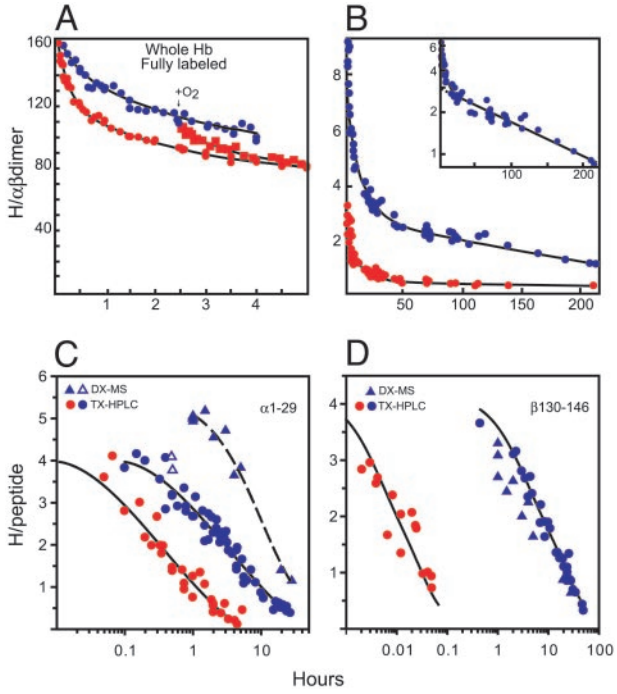

Fig. 1. Some allosterically sensitive hydrogens in Hb measured by tritium exchange and by DXMS (pH 7.4, 0°C); deoxy Hb is blue and Hb liganded by O_2 or CO is red. (*A*) Hb fully labeled by exchange-in in tritiated water was exchanged-out in oxy and deoxy forms, and with O_2 added back to exchanging deoxy Hb (45). (*B*) Illustration of functional labeling in an extreme case. Tritium exchange-in was for 1 min at pH 7.4, 0°C (oxy exchange-in/deoxy exchange-out is blue; the reverse process is red). (*Inset*) The difference curve after subtraction of the background is shown for deoxy Hb (46). (*C* and *D*). HX by functional labeling and HPLC fragment separation for the fragments α1–29 and β130–146, respectively. For tritium exchange experiments (filled circles), oxy Hb was initially labeled for 35 min at 0°C, pH 7.4 (24, 32). Triangles show comparative data from DXMS experiments, with oxy Hb initially labeled as just described (open triangles) or more intensively (filled triangles; 20 min, 20°C), which labels additional sensitive sites on α1–29. (HX rates within each set are not monoexponential because different amide hydrogens exchange with somewhat different intrinsic rate constants, k_{int} in Eq. **2**.)

the faster phase in *B*. The oxy/deoxy rate ratio (factors of 9-fold and 750-fold) indicate that these segments lose stabilizing interactions worth 1.2 kcal/mol and 3.6 kcal/mol in free energy, respectively, in the allosteric T to R transition (Eq. **4**).

These approaches are limited. Only four fragments have so far been cleanly isolated in this way (α1–29, ref. 32; α137–141, unpublished data; β86–102, ref. 31; and β130–146, ref. 24). HPLC alone cannot resolve the large number of fragments produced by relatively nonspecific acid proteases. Even for the accessible fragments, the results do not closely specify the amino acid positions of the sensitive sites.

Coverage. As have other workers before (10, 11), we supplemented the HPLC separation with a second dimension of fragment separation by online MS (ESI MS). The trace tritium label used before was replaced by deuterium and the liquid scintillation analysis for tritium label was replaced by mass analysis. To move toward single amino acid resolution, we obtained and studied multiple overlapping subfragments using two online immobilized protease columns with differing substrate specificity in tandem (pepsin, fungal protease XIII). The 100^+ fragments obtained with good yield and resolution provide redundant overlapping coverage of the entire amino acid sequence of both subunits (Fig. 2).

Published work using similar approaches has generally depended on a straightforward comparison of H-D exchange with and without the perturbation studied, analogous to Fig. 1*A*, although at the fragment level. As in Fig. 1*A*, the number of altered hydrogens and their rates in the two forms can then be ambiguous because of the undifferentiated background of functionally insensitive hydrogens. The functional labeling method used here overcomes this limitation by extracting only the functionally sensitive sites.

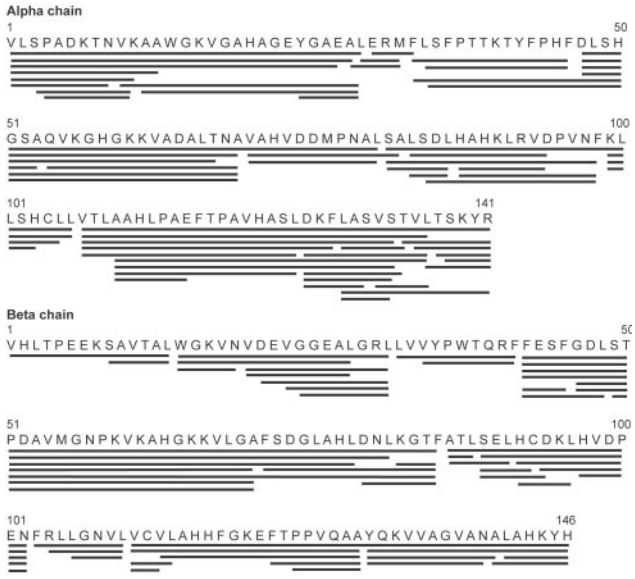

Fig. 2. MS fragments obtained reproducibly in good yield by using tandem online column-immobilized pepsin and fungal protease XIII.

A tradeoff is that the information obtained in any given experimental set is then limited to the portion of the overall HX curve within the selective exchange-in/exchange-out time window. A survey of functional labeling options led us to adopt a protocol for initial studies that uses exchange-in for 20 min at 20°C, pD_{read} 7.4, with exchange-out as before at 0°C, pH 7.4. Fig. 3 shows the number of hydrogens that are accessed by this labeling protocol. The upper curve in Fig. 3 shows the number of amide sites labeled in the whole Hb molecule when the protein was initially exchanged in as oxy Hb (20 min, 20°C) and then exchanged-out as deoxy Hb (0°C). Tritium exchange data obtained with this protocol exhibit ≈50 hydrogens per α-β dimer after 1 h of exchange-out. The DXMS results obtained by summing the fragment data described below (Fig. 4) are in good agreement. This curve is enriched in allosterically sensitive hydrogens but is still contaminated with some allosterically insensitive hydrogens.

The background curve in Fig. 3 (lower curve, deoxy-in/oxy-out), mainly shows the contribution of insensitive hydrogens. The difference between the upper curve (sensitive plus residual insensitive hydrogens) and the lower curve (largely insensitive hydrogens) gives the number of allosterically sensitive hydrogens that become measurable with this protocol. Some residual cross-contamination of the curves may exist, because of hydrogens that are only moderately sensitive (small rate ratio), or to a mismatch between exchange-in and exchange-out times, resulting in an underestimate of the number of sensitive sites. The ≈30 hydrogens found account for almost half of the 75 total allosterically sensitive sites enumerated in prior tritium exchange work (33), which used various exchange-in/exchange-out protocols to survey the entire Hb HX curve (≈260 amide hydrogens).

Resolution. Fig. 1 *C* and *D* compare some DXMS results to previous tritium exchange results for the fragments α1–29 and β130–146. When the same functional labeling protocol was used

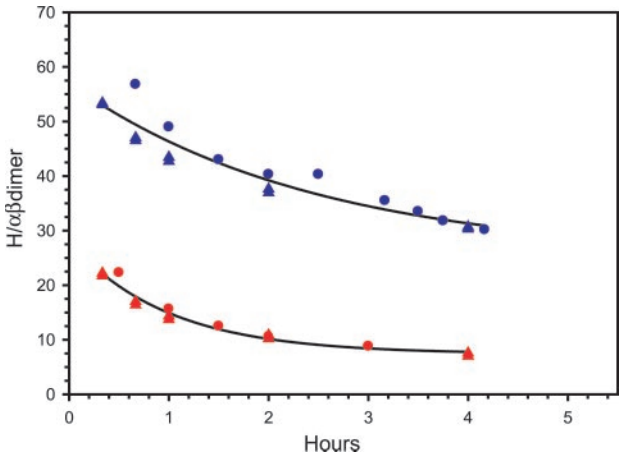

Fig. 3. The number of sites measured with the functional labeling protocol used (exchange-in 20°C, 20 min; exchange-out 0°C; upper curve in oxy/out deoxy; lower curve the reverse; pH or pD_{read} 7.4). Filled circles show exchange-out data measured in whole Hb by established tritium methods. Comparative DXMS results (filled triangles) show the summed deuterium labeling from the fragments in Fig. 4. Equilibrium isotope corrections were applied (29).

as before, good agreement was found. Also, as expected, the more intense exchange-in used in the DXMS work labeled additional allosterically sensitive sites on α1–29. It was known that the limited tritium exchange-in used before did not label the entire complement of sensitive hydrogens carried on α1–29 (ref. 32; the 20 min at 20°C exchange-in condition used is equivalent to >200 min at the 0°C condition used before).

Fig. 4 shows DXMS data for peptide fragments that span the entire length of both Hb subunits. Various HX patterns appear. A number of segments show no allosterically sensitive sites that exchange within the time window selected by the exchange-in/exchange-out protocol used. Some segments show one or two isolated sites, which may exchange by way of small structural fluctuations (30). Some other segments show larger sets of hydrogens. The hydrogens in each large set exchange at a similar rate in deoxy Hb and move in unison to a new faster rate when Hb changes from the T to the R form. This result suggests that each set is exposed to exchange by a concerted multiresidue local unfolding reaction. We focus here on the three sets of sensitive hydrogens studied before by tritium exchange.

***β*130–146.** The β-chain C terminus, captured on the fragment β130–146, makes allosterically sensitive intrasubunit and intersubunit links that account for half of the Bohr effect (34), help

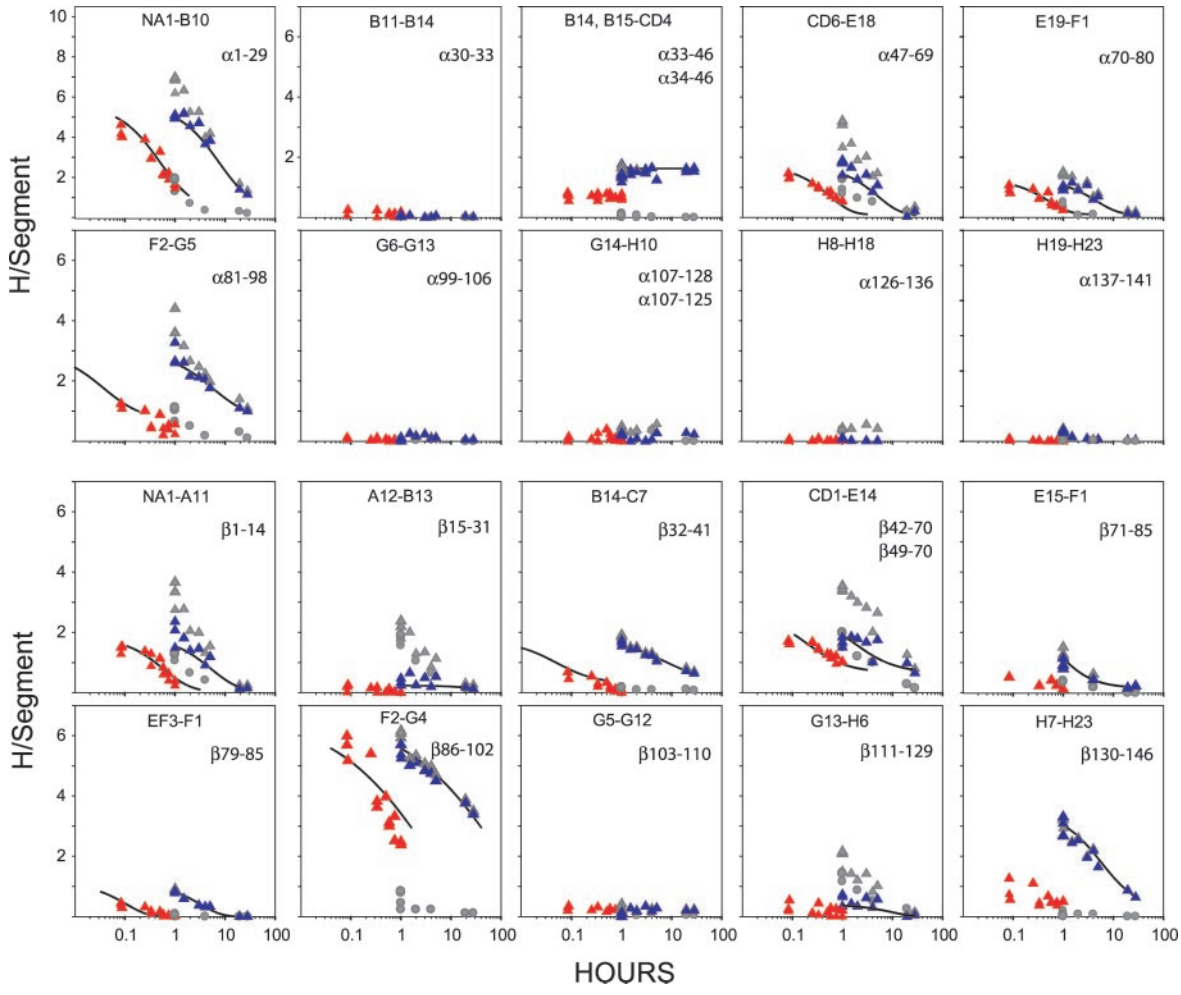

Fig. 4. DXMS results for fragments that span the entire α-chain and β-chain (exchange-in 20 min, 20°C; exchange-out at 0°C, pH or pD_{read} 7.4). Allosterically sensitive hydrogens in deoxy (blue) and liganded (red) Hb were obtained by subtracting the background from the raw data (both shown in gray). For liganded Hb, samples were initially exchanged out for 1 h in deoxy Hb to lose most of the background label, then switched to the liganded (R state) Hb by dilution into CO-containing buffer. The 1-h background was subtracted. Curves are drawn to fit the deoxy data, then moved onto the time axis to the oxy data to find the rate multiplication factor.

Table 1. DXMS results for β130–146 and subfragments

			Percent recovery		Mass increment			Zero time
Sequence	Mass	*Z*	Obs	$Theo_{10min}$	Obs	Bkgd	(Obs-bkgd)/ recov	Corrected ×1.25
β130–146	1868.01	1;3	86 (3)	78	2.6 (0.7)	0.0 (0.1)	3.2	4.0
β140–146	838.44	1;2	62 (4)	78	2.0 (0.4)	0.1 (0.2)	2.8	3.5
β141–146	767.41	1;2	60 (10)	72	1.7 (0.4)	0.1 (0.1)	2.4	3.0
β130–140	1118.61	1	87 (3)	82	0.3 (0.1)	0.0 (0.1)	0.3	0.4
β130–139	1047.57	1	86 (6)	85	0.3 (0.1)	0.1 (0.1)	0.3	0.4

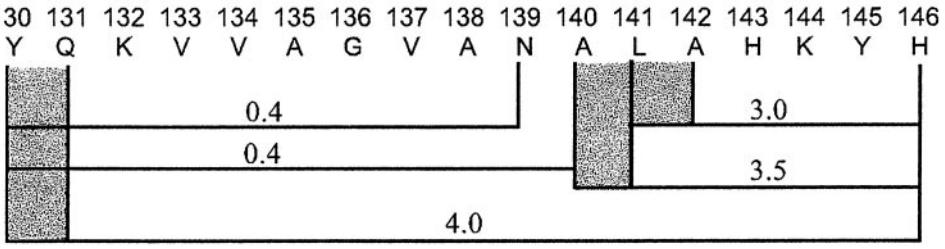

Initial columns specify the following: fragment ID, mass, and charge (*Z*), the fraction of D-label recovered in calibrating experiments with initially fully D-labeled Hb, and the theoretically calculated recovery (refs. 28 and 29; see spreadsheet at http://hx2.med.upenn.edu/download.html). Total analysis loss time at pH 2.3, 0°C, was 11 min, including thawing and proteolysis, with a total HPLC gradient of 10 min. Subsequent columns show the following: the number of carried deuterons after 1 h of deoxy Hb exchange-out for functionally labeled samples (obs), and for samples labeled in the reverse order to estimate the allosterically insensitive background contribution (bkgd). These data then yield the number of allosterically sensitive amide sites after 1 h of deoxy Hb exchange-out (recov is average of losses measured and expected). The final column shows the number of sensitive sites corrected to zero exchange-out time using the observed exchange-out rate (Figs. 1 and 3). Parentheses show the total range of variation for two to five independent runs. The fragment diagram summarizes the results. Shaded regions indicate that the N-terminal amino hydrogens for each fragment are always fully lost, as are exchangeable side-chain hydrogens. The penultimate amide NH is often largely lost, but less so when that residue has a large blocking side chain (Ile, Val, Leu, Trp, and Tyr; ref. 28).

to bind the allosteric effector bisphosphoglycerate (35) and participate in interactions that cross the allosterically important α_1–β_2 interface (36). This segment carries one of the two exceptionally sensitive sets of hydrogens seen before (Fig. 1*B*).

Table 1 shows data for the fragment β130–146 and four subfragments. The last column in Table 1 estimates the number of allosterically sensitive sites on each fragment at zero time of the DXMS analysis. This number has been corrected for the loss of label through the analysis and also during 1 h of deoxy Hb exchange-out before aliquots were taken for the DXMS analysis. (The 1-h exchange-out was used to chase the background of nonallosterically sensitive label, which is necessary for segments where the rate ratio between deoxy and oxy Hb is not large.)

The results place a concerted set of three to four allosterically sensitive amides on sequential residues at the β-chain C terminus and independently show ≈0 sensitive sites between Tyr-130 and Ala-140.

α1–29 and β86–102. Similar results are shown for the fragments α1–29 and β86–102 (see Tables 2 and 3, which are published as supporting information on the PNAS web site, www.pnas.org). In deoxy Hb, the α-chain makes allosterically sensitive interactions that involve residues near the N terminus of the α1–29 segment. β86–102 includes part of the β-chain F helix and the FG segment. The F helix includes the proximal histidine residue (F8), which ligands the heme. Residues in FG form allosterically sensitive interactions with the C-terminal segment (captured on β140–146).

Table 2 shows data for α1–29 and eight overlapping subfragments. The results detect six allosterically sensitive sites placed between residues 6 and 13. The helix (helix A) is continuously H-bonded between residue 6 and 18. Evidently, the N-terminal end of helix A participates in a reversible cooperative unfolding reaction that is promoted in the R state by 9-fold ($\Delta\Delta G^\circ$ = 1.2 kcal/mol).

Surprisingly, the number of hydrogens found does not account for all of the residues in the A helix, or even necessarily a wholly continuous string of sequential residues. This finding may be due to the tendency of the selective functional labeling method to underestimate the number of sensitive hydrogens. Alternative possibilities can be considered. The more C-terminal residues in the helix may not participate in the concerted unfolding. These or other residues within the group may participate but exchange by an additional faster pathway, and be lost during the chase time. Some sites may exchange more slowly and escape the initial labeling. Data error is a possibility, although run-to-run reproducibility is impressive.

Table 3 shows results for the fragment β86–102 and eight subfragments. Previous tritium exchange work found approximately seven allosterically sensitive hydrogens in this fragment, differing in rate between the T and R forms by a factor of 30 (37). The present results find approximately six allosterically sensitive sites, with a rate ratio of 25, between residues 89 (F5) and 98 (FG5).

Summary. These data associate three sets of allosterically sensitive hydrogens with known important structure changes and locate them at near amino acid resolution. Cooperative unfolding behavior is indicated, although the DXMS data do not precisely match the number of H-bonded amides in each segment. Whether this is due to methodological or data error or to other factors remains to be seen.

Discussion

The Free Energy of Structure Changes. Intramolecular signal transfer works by transducing and translocating structural free energy (see introduction). To understand these pathways, it will be necessary to connect the structure changes with the energy that they carry. Structural free energy and changes therein can only be obtained by measuring structural equilibria. If HX rates are determined by equilibrium unfolding reactions, then the structural stabilization free energy can be obtained as in Eq. **3** with some confidence, and

for change therein by Eq. **4**. This information can be connected in turn to the altered interactions known from crystallographic studies to impact on the segment measured.

To test the DXMS system, we focused here on three apparently concerted sets of hydrogens studied before by functional HX labeling using tritium exchange and HPLC fragment separation. Previous studies showed that the hydrogens in each set exchange at similar rates in deoxy T-state Hb. When all of the allosterically sensitive interactions are lost in liganded R-state Hb, each set of sensitive hydrogens moves as a group to a new rate, faster by 9-fold (32), 30-fold (37), and 750-fold (24). When specific mutations or chemical modifications are used to interdict individual allosterically sensitive interactions, the hydrogens in each affected HX set move to a common faster rate (19, 24, 38, 39). The same result occurs when particular heme sites are selectively liganded (40). Some changes in specific interactions evaluated before by these HX methods were found to match the free energies measured independently by their coupling to the subunit dissociation equilibrium (19). The present results come close to showing that the sensitive hydrogens in each HX set reside on sequentially placed residues.

These results consistently indicate that the changes in HX rate faithfully reflect changes in equilibrium local unfolding behavior. The measured change in HX rate for each set can therefore be used to parse out the free energy contribution of the allosterically important interactions (Eq. **4**).

Local Fluctuations Vs. Unfolding. The exploitation of naturally occurring HX behavior to locate and quantify functionally sensitive unfolding reactions can make it possible to track the pathway(s) of energy transfer through proteins. NMR studies of small proteins show that some hydrogens do exchange by way of sizable unfolding reactions and others can be induced to do so by imposing mildly destabilizing conditions (41). Several examples in Hb are documented here.

However, the reality of equilibrium unfolding reactions is often unclear. Many protein hydrogens appear to exchange by way of more local fluctuations, involving small structural distortions that deprotect one amino acid at a time (30). Some examples in Fig. 4 appear as isolated, although allosterically sensitive, hydrogens. Observations like this in Hb and other proteins indicate some kind of structural sensitivity, but may not reliably evaluate structural free energies, or even localize functionally important changes.

It can be noted that exchange by way of small fluctuations may be advantageous in some studies, for example in efforts to precisely define protein-binding sites. However the possibility of changes at a distance even when local fluctuations are at work, due for example to transmitted strain, needs to be evaluated (42, 43).

The factors that determine local fluctuational motions and concerted unfolding reactions remain to be elucidated (30, 44). In any case, the structural mode that provides the fastest exchange rate will dominate the exchange that is measured. The concerted sets of hydrogens studied here exchange at rates that are slower than fully exposed free amide rates by a protection factor of only $\approx 10^4$. Helical hydrogens that exchange by way of local fluctuations are often protected by larger factors. This finding may explain why the sets of hydrogens described here exchange by way of cooperative unfolding rather than through alternative local fluctuation pathways. The generality of this condition in Hb and other large proteins remains to be investigated.

HX Analysis. Crystallographic and NMR methods now easily provide pictures of protein structures. This kind of information is indispensable for molecular studies. HX approaches seem able to fill in the dynamic and energetic dimensions of these pictures and thus contribute to a more profound understanding of how proteins function. Toward this goal, previous work (6) demonstrated the HX functional labeling and fragment separation techniques for protein structural studies. Results obtained here and in other publications demonstrate the potential of adding an automated high-throughput, high-resolution MS capability.

We recognize the indispensable scientific contributions of Joan J. Englander to this and prior work, and we mourn her loss. We thank David Smith, David Wemmer, and Dennis Pantazatos for their valuable help. This work was supported by grants from the National Institutes of Health and the Mathers Foundation (to S.W.E.), and the University of California BioStar and LSI programs, Grants S97-90, S99-44, and L98-30 (to V.L.W.). ExSAR Corporation is a sponsor. V.L.W. and Y.H. have financial interests in and S.W.E. is a consultant to ExSAR Corporation.

1. Woodward, C. K. (1994) *Curr. Opin. Struct. Biol.* **4,** 112–116.
2. Scholtz, J. M. & Robertson, A. D. (1995) *Methods Mol. Biol.* **40,** 291–311.
3. Englander, S. W., Sosnick, T. R., Englander, J. J. & Mayne, L. (1996) *Curr. Opin. Struct. Biol.* **6,** 18–23.
4. Raschke, T. M. & Marqusee, S. (1998) *Curr. Opin. Biotechnol.* **9,** 80–86.
5. Rogero, J. R., Englander, J. J. & Englander, S. W. (1986) *Methods Enzymol.* **131,** 508–517.
6. Englander, S. W. & Englander, J. J. (1994) *Methods Enzymol.* **232,** 26–42.
7. Rosa, J. J. & Richards, F. M. (1979) *J. Mol. Biol.* **133,** 399–416.
8. Englander, S. W., Calhoun, D. B., Englander, J. J., Kallenbach, N. R., Liem, R. K. H., Malin, E. L., Mandal, C. & Rogero, J. R. (1980) *Biophys. J.* 577–590.
9. Englander, J. J., Rogero, J. R. & Englander, S. W. (1985) *Anal. Biochem.* **147,** 234–244.
10. Zhang, Z. & Smith, D. L. (1993) *Protein Sci.* **2,** 522–531.
11. Hoofnagle, A. N., Resing, K. A. & Ahn, N. G. (2003) *Annu. Rev. Biophys. Biomol. Struct.* **18,** in press.
12. Woods, V. L., Jr., & Hamuro, Y. (2001) *J. Cell. Biochem. Suppl.* **37,** 89–98.
13. Woods, V. L., Jr. (1997) U.S. Patent 5,658,739.
14. Woods, V. L., Jr. (2001) U.S. Patent 6,291,189.
15. Woods, V. L., Jr. (2001) U.S. Patent 6,331,400.
16. Hamuro, Y., Burns, L., Canaves, J., Hoffman, R., Taylor, S. & Woods, V. L., Jr. (2002) *J. Mol. Biol.* **321,** 703–714.
17. Hamuro, Y., Wong, L., Shaffer, J., Kim, J. S., Stranz, D. D., Jennings, P. A., Woods, V. L., Jr., & Adams, J. A. (2002) *J. Mol. Biol.* **323,** 871–881.
18. Hamuro, Y., Zawadzki, K. M., Kim, J. S., Stranz, D. D., Taylor, S. S. & Woods, V. L., Jr. (2003) *J. Mol. Biol.* **327,** 1065–1076.
19. Englander, S. W., Englander, J. J., McKinnie, R. E., Ackers, G. K., Turner, G. J., Westrick, J. A. & Gill, S. J. (1992) *Science* **256,** 1684–1687.
20. Holt, J. M. & Ackers, G. K. (1995) *FASEB J.* **9,** 210–218.
21. Ackers, G. K. (1998) *Adv. Protein Chem.* **51,** 185–253.
22. Ackers, G. K., Dalessio, P. M., Lew, G. H., Daugherty, M. A. & Holt, J. M. (2002) *Proc. Natl. Acad. Sci. USA* **99,** 9777–9782.
23. Englander, S. W., Calhoun, D. B. & Englander, J. J. (1987) *Anal. Biochem.* **161,** 300–306.
24. Louie, G., Thao, T., Englander, J. J. & Englander, S. W. (1988) *J. Mol. Biol.* **201,** 755–764.
25. Jeng, M.-F. & Englander, S. W. (1991) *J. Mol. Biol.* **221,** 1045–1061.
26. Englander, S. W. & Kallenbach, N. R. (1984) *Q. Rev. Biophys.* **16,** 521–655.
27. Hvidt, A. & Neilson, S. O. (1966) *Adv. Protein Chem.* **21,** 287–386.
28. Bai, Y., Milne, J. S., Mayne, L. & Englander, S. W. (1993) *Proteins Struct. Funct. Genet.* **17,** 75–86.
29. Connelly, G. P., Bai, Y., Jeng, M. F., Mayne, L. & Englander, S. W. (1993) *Proteins Struct. Funct. Genet.* **17,** 87–92.
30. Maity, H., Lim, W. K., Rumbley, J. N. & Englander, S. W. (2003) *Protein Sci.* **12,** 153–160.
31. Englander, J. J., Rogero, J. R. & Englander, S. W. (1983) *J. Mol. Biol.* **169,** 325–344.
32. Ray, J. & Englander, S. W. (1986) *Biochemistry* **25,** 3000–3007.
33. Malin, E. L. & Englander, S. W. (1980) *J. Biol. Chem.* **255,** 10695–10701.
34. Perutz, M. F., Gronenborn, A. M., Clore, G. M., Fogg, J. H. & Shih, D. T. (1985) *J. Mol. Biol.* **183,** 491–498.
35. Arnone, A. (1972) *Nature* **237,** 146–149.
36. Perutz, M. F., Wilkinson, A. J., Paoli, M. & Dodson, G. G. (1998) *Annu. Rev. Biophys. Biomol. Struct.* **27,** 1–34.
37. Englander, J. J., Rogero, J. R. & Englander, S. W. (1983) *J. Mol. Biol.* **63,** 153–169.
38. Louie, G., Englander, J. J. & Englander, S. W. (1988) *J. Mol. Biol.* **201,** 765–772.
39. Englander, J. J., Louie, G., McKinnie, R. E. & Englander, S. W. (1998) *J. Mol. Biol.* **284,** 1695–1706.
40. Englander, J. J., Rumbley, J. N. & Englander, S. W. (1998) *J. Mol. Biol.* **284,** 1707–1716.
41. Englander, S. W. (2000) *Annu. Rev. Biophys. Biomol. Struct.* **29,** 213–238.
42. Benjamin, D. C., Williams, D. C., Smith-Gill, S. J. & Rule, G. S. (1992) *Biochemistry* **31,** 9539–9545.
43. Hilser, V. J., Dowdy, D., Oas, T. G. & Freire, E. (1998) *Proc. Natl. Acad. Sci. USA* **95,** 9903–9908.
44. Milne, J. S., Mayne, L., Roder, H., Wand, A. J. & Englander, S. W. (1998) *Protein Sci.* **7,** 739–745.
45. Englander, S. W. & Mauel, C. (1972) *J. Biol. Chem.* **247,** 2387–2394.
46. Liem, R. K. H., Calhoun, D. B., Englander, J. J. & Englander, S. W. (1980) *J. Biol. Chem.* **255,** 10687–10694.